Wave separation and pipeline condition assessment using in-pipe fibre optic pressure sensors

He Shi, Jinzhe Gong, Peter R. Cook, John W. Arkwright, Gretel M. Png, Martin F. Lambert, Aaron C. Zecchin and Angus R. Simpson

ABSTRACT

The use of two pressure transducers in close proximity can enable the separation of the directional travelling pressure waves in pipelines. However, the implementation of this measurement strategy in real water pipes is difficult due to the lack of closely located access points. This paper reports the use of a customised in-pipe fibre optic pressure sensor array for hydraulic transient wave separation and pipeline condition assessment. The fibre optic pressure sensor array can be inserted into a pressurised pipeline through a single access point. The array consists of multiple fibre Bragg grating (FBG)-based pressure sensors in close proximity (~0.5 m apart). A previously developed wave separation algorithm is adapted to analyse the transient pressure measurement from the FBG sensors. The resultant directional pressure waves are then used to detect pipe sections with a thinner wall thickness. A challenge is the influence of the in-pipe fibre optic sensing cable on the transient pressure measurement. The impact is analysed and adjustments to the pipeline condition assessment algorithm are undertaken to resolve the issue. The successful experimental application verifies the usefulness of the in-pipe fibre optic sensor array, which can facilitate transient-based pipeline condition assessment for buried water pipes with limited access points.

Key words | hydraulic transient, optic fibre, pipeline condition assessment, water hammer, wave separation

He Shi
Jinzhe Gong (corresponding author)
Gretel M. Png
Martin F. Lambert
Aaron C. Zecchin
Angus R. Simpson
School of Civil, Environmental and Mining Engineering,
University of Adelaide,
SA 5005, Adelaide,
Australia
E-mail: *jinzhe.gong@adelaide.edu.au*

Peter R. Cook
John W. Arkwright
School of Computer Science, Engineering and Mathematics,
Flinders University,
1284 South Road, Clovelly Park, SA 5042,
Australia

INTRODUCTION

Water utilities globally are facing the problem of ageing water distribution systems (WDSs), and the cost of maintenance and replacement is predicted to explode under current practice. For instance, it is estimated that more than US$1 trillion will be required between 2011 and 2035 to replace ageing water mains and address projected growth (American Water Works Association 2012). Pipeline condition assessment has becoming increasingly important, because the actual condition of pipelines can help strategically prioritise investment and extend asset life.

Among many pipeline condition assessment techniques available, hydraulic transient-based methods are particularly attractive because they can achieve continuous pipe wall condition assessment for hundreds of metres up to kilometres of pipe in a single test (Stephens *et al.* 2013). The approach uses small controlled hydraulic transient pressure waves, which travel at about 1,200 m/s in pressurised metallic water pipes, and will induce wave reflections at pipe cross-sections with physical changes (e.g., leaks, blockages and wall thinning due to corrosion), and the reflections can be interpreted by appropriate algorithms to reveal the nature of the anomaly (Chaudhry 2014). In addition to pipe wall condition assessment (Zeng *et al.* 2018; Zhang *et al.* 2018), many transient-based techniques have been developed for the detection of leaks (Brunone & Ferrante 2001; Covas *et al.* 2005; Shamloo & Haghighi 2009; Soares *et al.* 2011;

doi: 10.2166/hydro.2019.051

Gong *et al.* 2013a; Duan 2016), blockages (Sattar *et al.* 2008; Meniconi *et al.* 2013; Massari *et al.* 2014), illegal branches (Meniconi *et al.* 2011), general anomaly screening (Meniconi *et al.* 2015) or system parameter identification (Zecchin *et al.* 2014).

In operational pipe systems, pressure sensors are installed at existing access points (Ghazali *et al.* 2012; Gong *et al.* 2015), such as air valves or fire hydrants, which are typically hundreds of metres apart from each other, to avoid excavation or tapping. For any interior point along a pipe, the measurement from a single pressure sensor is always the superimposed amplitude of the pressure waves travelling upstream and downstream. As a result, it is difficult to tell whether a measured pressure reflection is from the upstream or downstream side of the transducer, or actually a combination of waves from both sides. The use of measurements from multiple access points (hundreds of metres apart) and a time-shifting technique (Gong *et al.* 2016) is helpful in providing the directional information, but only when the reflected waves are simple in wave form and limited in number (i.e., the pipeline configuration and condition are not complex).

A wave separation technique recently developed for hydraulic transient pressure waves in pipelines has provided a robust solution to obtain the directional information of wave reflections (Shi *et al.* 2017). The wave separation technique uses two pressure sensors in close proximity along a pipe (in the scale of metres), and they are referred to as a 'dual-sensor'. It was adapted to water pipe systems from the original technique for separating directional acoustic waves using multiple microphones (Chung & Blaser 1980). In the wave separation technique, the time–domain pressure reflection signals as measured by the dual-sensor are transformed into the frequency domain, processed based on the fact that a directional wave arrives at the two sensors at different times but with a specific time delay, and then transformed back into the time domain. The results are two directional pressure waves with significantly reduced complexity, in which any major wave reflection can be attributed to its source by the principle of time–domain reflectometry. One practical challenge of this wave separation technique in buried water pipelines, however, is the difficulty in achieving the dual-sensor measurement configuration.

To address this challenge, the authors have developed in-pipe fibre optic transient pressure sensors, with the first generation tested in the laboratory for proof-of-concept (Shi *et al.* 2015) and the second generation tested and reported in this paper for wave separation and pipe condition assessment. The optic pressure sensors are based on fibre Bragg gratings (FBGs), and multiple sensors are placed in close proximity (~0.5 m) in a protective cable. The sensor cable, with a diameter of ~4 mm, can be inserted into a pipeline through a single access point. Laboratory experiments are conducted in a single copper pipeline with two short sections in thinner wall thicknesses, and the wave separation technique is applied to the measured transient pressure data for pipe wall condition assessment purpose. One particular challenge is the impact of the sensor cable on the transient response. The sensor design, the impact of the sensor cable, the wave separation and the application to pipe wall condition assessment are discussed in the following sections.

IN-PIPE FIBRE OPTIC TRANSIENT PRESSURE SENSOR ARRAY

The in-pipe fibre optic sensor array used in this research includes five FBG-based pressure sensors (FBG1 to FBG5) in a 5.37 m long cable, the schematic of which is given in Figure 1. It is a further development based on the FBG manometry catheter developed by Arkwright *et al.* (2012) for measuring muscular activity in the human gut. The distance between FBG1 and FBG2 is 0.725 m and that for the rest is 0.5 m. The cable that protects the optical fibre is made from plastic material, and has a diameter of approximately 4 mm. At each FBG pressure sensor, a 10 mm window is open in the protective cable, and a flexible elastomeric sleeve is used to cover the FBG, as illustrated in Figure 2.

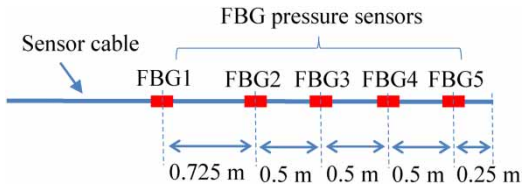

Figure 1 | Schematic of the in-pipe fibre optic sensor cable.

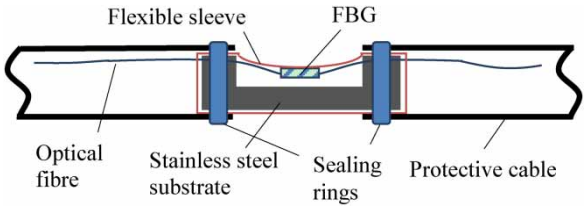

Figure 2 | Schematic of the FBG pressure sensor.

The FBG is designed to have a downward arc under atmosphere pressure and the flexible sleeve is in close contact with the sensor. As the pressure increases from atmosphere pressure, the sleeve presses the FBG further downwards, which causes a change in the strain and in turn a shift in the reflected wavelength of the FBG. This configuration, in particular the arc-shaped pre-load, is a new design compared with its predecessor reported in Shi *et al.* (2015), and it enables high sensitivity to pressure variations under high background pressure condition (as is the case in pressurised water pipes). This in-pipe fibre optic sensor array has recently been applied to measure leak-induced hydraulic noise in the steady state and wave reflections under transient events (Gong *et al.* 2018).

LABORATORY EXPERIMENTS

Experimental apparatus

Laboratory experiments have been conducted to assess the usefulness of the in-pipe fibre optic sensor array in transient pressure wave separation and pipe wall condition assessment. The layout of the experimental pipeline systems is given in Figure 3.

The laboratory system was a copper pipe that consisted of mainly Class A pipe sections and two short sections in Class B and C, respectively. The Class B and C sections have a thinner wall thickness and were used to simulate deteriorated pipe sections (e.g., extended corrosion). The length information of the pipeline system is shown in Figure 3 and the physical details of pipes in different classes are given in Table 1, where D, e, a and B represent internal diameter, wall thickness, wave speed and impedance, respectively, and the subscripts A, B, and C represent pipe Class A, B and C, respectively. Pipe impedance B is defined as:

$$B = \frac{a}{gA} \tag{1}$$

in which g is the gravitational acceleration, and A is the cross-sectional area of the pipe section under consideration.

Two conventional pressure transducers (T1 and T2 in Figure 3, M5HB, Keller AG, Switzerland) were flush mounted on the pipe wall through small brass blocks encasing the pipe. A solenoid-controlled side-discharge valve was used as the transient wave generator (G), and it was installed at the same cross-section of the pipe where T1 was located. The solenoid valve was installed on the top of the pipe for water discharge and the release of any trapped air. The transducers were installed on the side and with an upward angle to prevent any air from being trapped at the sensor head. The fibre optic sensor cable was inserted into the pipeline through an angled tapping point and sealed with an

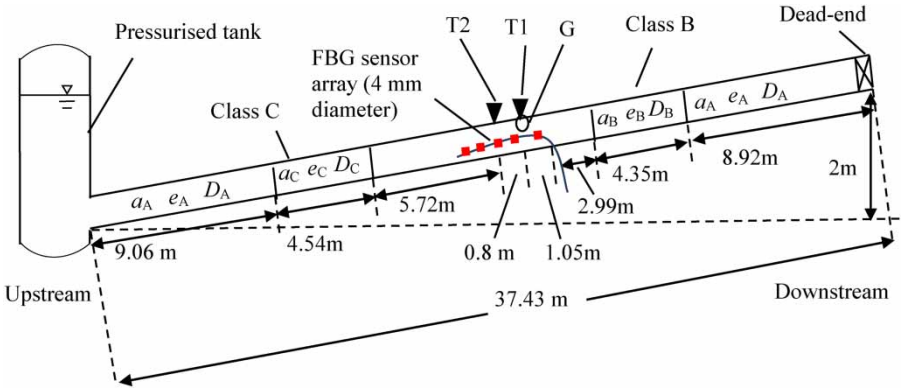

Figure 3 | Layout of the experimental pipeline system.

Table 1 | Physical details of the pipeline system used in the laboratory experiments

Pipe class	Internal diameter (mm)	Wall thickness (mm)	Wave speed (m/s)	Impedance (s/m^2)
A	$D_A = 22.14$	$e_A = 1.63$	$a_A = 1{,}319$	$B_A = 349{,}000$
B	$D_B = 22.96$	$e_B = 1.22$	$a_B = 1{,}273$	$B_B = 314{,}000$
C	$D_C = 23.58$	$e_C = 0.91$	$a_C = 1{,}217$	$B_C = 284{,}000$

O-ring gland. The insertion point is 1.05 m away from the transient generator G and transducer T1. The optical fibre was illuminated using a super-luminescent light emitting diode (DL-BP1-1501A, DenseLight, Singapore) and the reflected wavelengths from the sensor array were monitored using a solid-state spectrometer (I-MON 512 HS, Ibsen Photonics, Denmark). Transducer T2 and FBG3 were placed at the same location, and as a result, the overall length of the fibre optic cable inside the pipeline is 3.1 m. The sampling rate for the FBG sensors was 12.376 kHz and that for the conventional sensors was 20 kHz.

Pressure measurements and simulations

In the initial steady-state condition, the pipeline system was pressurised at 3 bar by the pressurised tank, and the solenoid valve was fully open to discharge water. The solenoid valve was then abruptly closed, which resulted in two identical incident step waves propagating along the pipe in two directions.

The pressure measurements from T2 and FBG3 are shown in Figure 4, together with the measurement from T2 when no fibre optic cable was present, and with the numerical pressure response at T2 obtained by the method of characteristics (MOC). In the MOC simulation, a pipe model is established based on the information in Figure 3 and Table 1 for the scenario that the fibre optic sensor cable is present. The wave speed in the pipe section where the fibre cable is enclosed is 1,230 m/s as determined from the laboratory measurements, and this is used in the numerical model. The time step used in the simulation is 0.5 ms. Steady friction with a Darcy–Weisbach frictional factor of 0.02 is considered.

The incident wave and the major wave reflections from key features are highlighted in Figure 4. According to the principle of time-domain reflectometry (TDR), once a wave

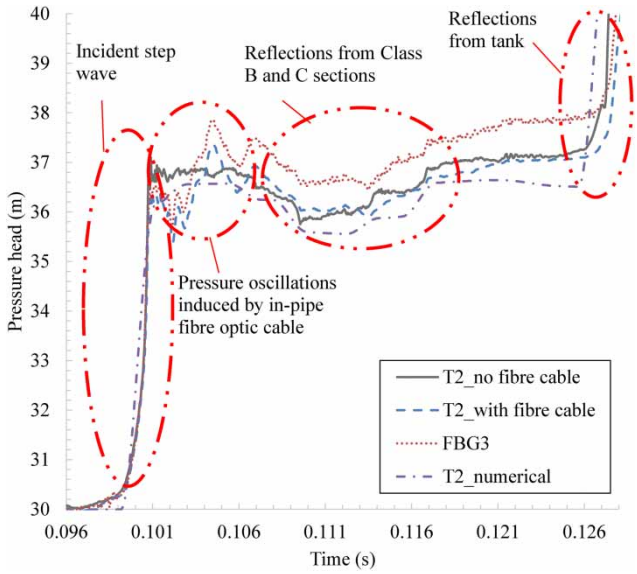

Figure 4 | Transient pressure responses from conventional sensor T2 (laboratory results with and without the present of fibre sensor cable, and numerical results) and from fibre optic sensor FBG3 (fibre sensor cable in pipe).

front encounters a physical discontinuity (e.g., a wall thickness change), reflections occur and propagate backwards. Reflections from features closer to the generator will arrive at the transducer (at the same or close location of the generator) sooner. The short duration of the wave front ensures a high spatial resolution. Based on the analysis in Gong *et al.* (2013b), for a step wave with an effective rise time of T_r and a wave speed of a, reflections from two discontinuities with a distance of $T_r a/2$ or larger are distinguishable from each other. The effective rise time of the incident step wave in this study is about 2 ms as shown in Figure 4. Considering the highest wave speed of 1,319 m/s as in Table 1, the spatial resolution is about 1.32 m. The distance between any two major physical discontinuities is larger than this threshold in the experimental system (Figure 3), therefore the major reflections can be identified with confidence, especially after the wave separation, as discussed later.

It can be seen from Figure 4 that the presence of the in-pipe fibre optic sensor cable changes the transient pressure response of the pipeline system. The impact of the cable mainly manifests as pressure oscillations in a short time period after the generation of the incident wave. The pressure oscillations are attributed to the in-pipe cable together with the tapping point for cable insertion, which change the local impedance of the pipeline. Using the

experimentally determined wave speed of 1,230 m/s and Equation (1), and considering the small change in the pipe cross-sectional area (the cross-sectional area of cable is about 3% that of the pipe, but the cable area may be compressed to be even smaller under pressure), the impedance of the pipe section with the in-pipe fibre optic cable is calculated as 337,000 s/m^2, which is smaller than the impedance of normal Class A pipe. The pressure signal seems complex in the original measurement as shown in Figure 4 but will become clearer after the wave separation, as discussed later.

Combined pressure wave reflections from the Class B and C sections are also recorded in the traces in Figure 4. The laboratory measurements from both T2 and FBG3 when the in-pipe cable was present are slightly smoother than that from T2 when no cable was in the pipe. The effect of signal smoothness is most likely due to the viscoelasticity of the plastic material.

Overall, those three experimental traces are generally consistent, and they are also consistent with the numerical results. Since the length of the cable inside the pipe is short (3.1 m), the pressure oscillations induced by the cable are confined in a very short time period (~5 ms) after the generation of the incident wave and the effect of signal smoothness is insignificant.

WAVE SEPARATION

Directional pressure waves

The pressure measurements from FBG2 and FBG3, as shown in Figure 5, are used for wave separation. They are close to the transient generator and the results can be compared with those obtained from the conventional sensors (T1 and T2). The procedure of the wave separation follows that outlined in Shi *et al.* (2017). The short-duration wave fronts of the incident step wave as measured by FBG2 and FBG3 (as shown in Figure 5) are extracted and used to empirically calibrate the transfer function for the short pipe section between the two sensors. The transfer function describes how the wave evolves over propagation, and includes information about the wave speed and wave attenuation. The wave reflections before the arrival of the tank-induced reflection are extracted and put into the wave separation algorithm. The results of the

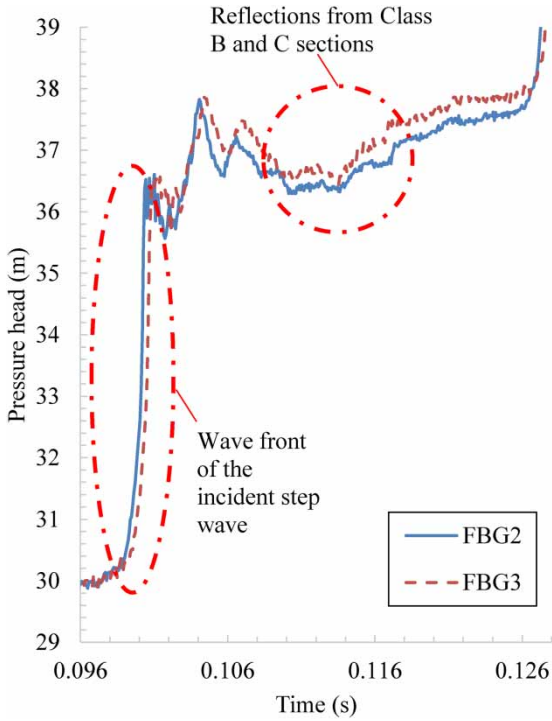

Figure 5 | Transient pressure measurements from FBG2 and FBG3.

directional pressure reflection waves experimentally extracted from the FBG sensors and the conventional sensors are given in Figure 6. The wave separation algorithm is also applied to the numerically simulated pressure responses and the results are shown in Figure 6 for comparison. Note that the directional pressure waves are normalised by the size of the incident wave for ease of comparison.

Figure 6 demonstrates that the major reflections from the Class B and Class C sections have been separated using the experimental data from either the FBG sensors or the conventional sensors, and the experimental results are consistent with the numerical results. The wave separation decomposes the superimposed raw pressure measurement into directional pressure waves, simplifies the complexity of the signal, and enables better understanding of the source of reflections. Discrepancies exist and are discussed in the following sub-section.

Discussion

The experimentally determined directional waves using the FRB sensors and the conventional sensors are highly consistent in the wave form. For the wave reflections from the

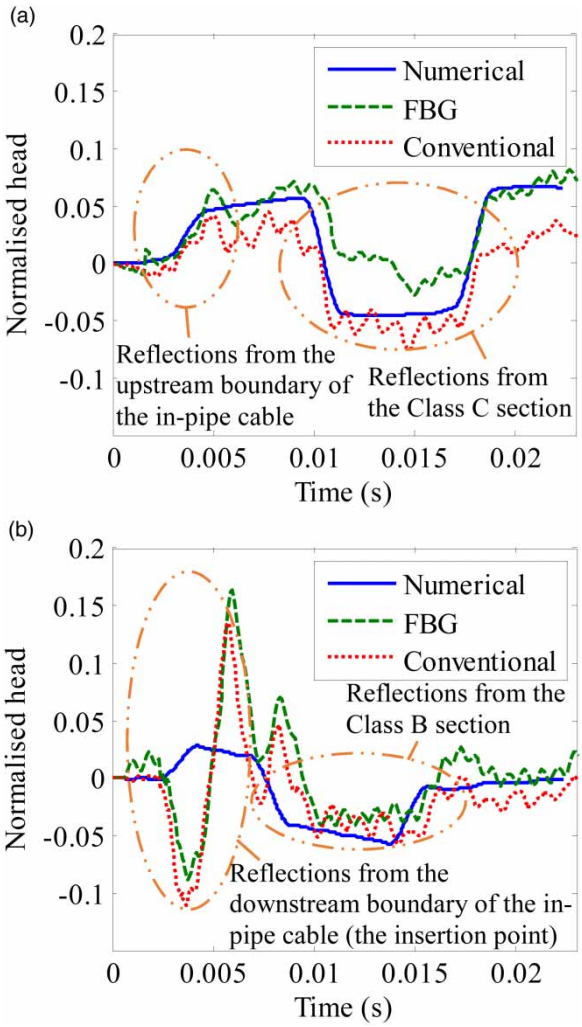

Figure 6 | Wave separation results obtained from numerical simulations, fibre optic sensors (FBG2 and FBG3) and conventional sensors (T1 and T2): (a) wave reflections from the upstream side of the dual-sensor and propagating towards the dead-end; and (b) wave reflections from the downstream side of the dual-sensor and propagating towards the tank.

upstream side of the dual-sensor and propagating towards the dead-end (Figure 6(a)), the experimental results are also highly consistent with the numerical results. The first step rise is the reflection from the upstream boundary of the in-pipe cable, and it is because the pipe section (Class A) with the cable has a lower impedance than that in normal Class A pipe sections. The cable is made from plastic material, which is much lower in strength compared to the material of the pipe wall (copper), and it results in a lower wave speed and therefore a lower impedance for the pipe section hosting the cable. When a positive wave is propagating from a lower impedance pipe section to a higher impedance one, a positive pressure wave reflection will occur (Wylie 1983). The following step drop and then step rise are reflections from the Class C pipe section, which has an impedance lower than the Class A pipe. A detailed explanation of the wave reflection mechanism from a short pipe section with a different impedance can be found in Gong *et al.* (2013b). The experimental results have some small oscillations in addition to the major reflections. The oscillations can result from the transient interference induced by the vibration of the solenoid valve at the sudden closure, and the uncertainty in the empirical determination of the transfer function. The numerical results are smooth and clearly show the expected reflections, which confirms the effectiveness and accuracy of the wave separation algorithm itself.

For the wave reflections from the downstream side of the dual-sensor and propagating towards the tank (Figure 6(b)), the reflections from the Class B section (as highlighted in the figure) are generally consistent for the three sets of results; however, discrepancies are observed between the experimental and the numerical results for the reflections from the downstream boundary of the in-pipe cable (which was the cable insertion point). The experimental results show a negative reflection followed by a positive reflection and some wave oscillations, while the numerical results show a step response similar to the upstream-boundary reflection as seen in Figure 6(a). The insertion tapping point (an angled conduit in a brass block) was sealed by an O-ring gland with a 'finger-tight' condition. The conduit and the O-ring seal are likely to respond to pressure transients like a small accumulator, thus producing the signature of a negative reflection followed by a positive reflection as observed in the experimental results. The numerical model did not include this complexity, therefore the numerical result only shows the step reflection as induced by an impedance change at the downstream-boundary of the in-pipe cable.

PIPE WALL CONDITION ASSESSMENT

Methodology

The original direct-reflection analysis-based condition assessment technique (Gong *et al.* 2013b) needs to be further developed for the directional waves obtained from the

in-pipe fibre optic sensor array. The original condition assessment algorithm assumes that the incident wave is generated and the pressure responses are measured in an intact pipe section, and the deteriorated sections are limited in number and mild in deterioration. In the case of using the in-pipe fibre optic sensor cable, the generation of the incident wave and the pressure measurement are undertaken in the section that encloses the cable, and the impedance of this section is considerably lower than that in normal intact pipe sections. However, the same principle still applies. That is, when a pressure wave propagates from the ith pipe section to the $(i+1)$th pipe section where the impedance changes, the sign-sensitive amplitude of the normalised wave reflection (equivalent to the reflection coefficient) and that of the normalised transmitted wave (equivalent to the transmission coefficient) are related to the impedance of the two sections (Wylie 1983; Gong *et al.* 2013b), as given in Equations (2) and (3), respectively:

$$R_{i,i+1} = \frac{B_{i+1} - B_i}{B_{i+1} + B_i} \tag{2}$$

$$T_{i,i+1} = \frac{2B_{i+1}}{B_{i+1} + B_i} = 1 + R_{i,i+1} \tag{3}$$

where $R_{i,i+1}$ and $T_{i,i+1}$ are the reflection and transmission coefficient, respectively, for a wave propagating from the ith to the $(i+1)$th pipe section.

The relationships shown in Equations (2) and (3) are the same as the reflection and transmission coefficients defined in acoustic reflectometry (Sharp 1996), where typically acoustic waves propagating in air and in a wave guide are considered. Considering an incident wave generated at section 1 and only propagating towards one direction (as in the case of directional waves as previously discussed), the normalised initial reflection from the nth section as would be measured in the first section can be derived as:

$$R_{1,n} = R_{n-1,n} \prod_{i=1}^{n-2} (1 - R_{i,i+1}^2) \tag{4}$$

Application and verification

To verify the modified condition assessment algorithm as discussed in the previous section, Equation (4) is applied to the directional pressure wave coming from the upstream side of the dual-sensor and propagating towards the dead-end (Figure 6(a)). Rearranging Equation (2), the impedance of the $(i+1)$th section can be calculated by:

$$B_{i+1} = B_i \frac{1 + R_{i,i+1}}{1 - R_{i,i+1}} \tag{5}$$

The pipe section with the FBG sensor cable inside can be considered as the first section, the normal Class A section on the upstream side is the second section, and the Class C section is the third section. The reflection coefficients $R_{1,2}$ and $R_{1,3}$ can be determined from the sign-sensitive amplitude of the major wave reflections in the directional wave shown in Figure 6(a). The reflection coefficient $R_{2,3}$ can then be calculated by Equation (4). Finally, Equation (5) can be used to calculate B_3, which, in this case, is the impedance of the Class C section B_C. Table 2 summarises the results. Note that, although three significant figures are used for the values, the reflection coefficients (i.e., the amplitude of the normalised reflections) are determined manually and uncertainties are involved.

It can be seen from Table 2 that the determined impedance values for the Class C section are consistent with the calculated theoretical value of B_C as given in Table 1 (284,000 s/m^2), which verifies that pipeline condition assessment can be conducted using the in-pipe fibre optic sensors with the methodology presented. The values of $R_{2,3}$ are very close to those of $R_{1,3}$, which demonstrates that the local impedance change induced by the in-pipe sensor cable has an insignificant impact on the pipeline condition assessment. The discrepancies between the determined impedance values and the theoretical value are mainly due

Table 2 | Pipe impedance determined from the directional pressure wave coming from the upstream side of the dual-sensor and propagating towards the dead-end (Figure 6(a))

Cases	Reflection coefficient $R_{1,2}$	Reflection coefficient $R_{1,3}$	Reflection coefficient $R_{2,3}$	Determined impedance B_C (s/m^2)
Numerical	0.040	−0.10	−0.10	285,000
FBG	0.0588	−0.0962	−0.0965	287,000
Conventional	0.0497	−0.110	−0.110	280,000

to the error associated with the wave separation, uncertainties in the determined amplitude of wave reflections and uncertainties in the pipeline parameters used to calculate the theoretical value.

CONCLUSIONS

A customised in-pipe fibre optic pressure sensor array has been used in the laboratory for hydraulic transient wave separation and pipeline condition assessment. The in-pipe fibre optic sensor array consists of five FBG-based pressure sensors in close proximity. The optic fibre is protected by a plastic cable with a diameter ~4 mm and the cable can be inserted into a pressurised pipeline through a single tapping point. With empirical calibration of the transfer function of the short pipe section between two sensors, a previously developed wave separation technique is successfully implemented on the transient pressure data measured from the fibre optic sensors, and the resultant directional waves are consistent with those obtained from conventional pressure sensors.

The impact of the in-pipe fibre optic sensor cable to the transient pressure response of the pipeline system has been assessed and discussed based on the directional pressure waves. The in-pipe sensor cable, as made from a plastic material, reduces the local pipe impedance and therefore introduces wave reflections. It also slightly smoothens the transient pressure signal. The entrance point of the cable acts like a small accumulator and introduces pressure oscillations. However, overall, the impact of the in-pipe cable is moderate because of its short length, and it does not impede the application of transient pressure measurement for pipeline condition assessment.

A direct wave-reflection analysis-based pipeline condition assessment algorithm has been further developed to incorporate the impact of the local impedance change induced by the in-pipe cable. The impedance of a Class C pipe section, which has a thinner wall thickness to simulate a deteriorated section, has been determined from the previously obtained directional waves, and the results are consistent with the theoretical value.

The results have verified the usefulness of the in-pipe fibre optic sensor array for hydraulic transient wave separation and pipeline condition assessment. The in-pipe sensor cable provides the ability to have multiple pressure measurements through one access point.

ACKNOWLEDGEMENTS

The research presented in this paper has been supported by the Australia Research Council through the Discovery Project Grant DP170103715.

REFERENCES

American Water Works Association 2012 *Buried No Longer: Confronting America's Water Infrastructure Challenge*. AWWA, Denver, CO, USA.

Arkwright, J. W., Blenman, N. G., Underhill, I. D., Maunder, S. A., Spencer, N. J., Costa, M., Brookes, S. J., Szczesniak, M. M. & Dinning, P. G. 2012 Measurement of muscular activity associated with peristalsis in the human gut using fiber Bragg grating arrays. *IEEE Sensors J.* **12** (1), 113–117.

Brunone, B. & Ferrante, M. 2001 Detecting leaks in pressurised pipes by means of transients. *J. Hydraulic Res.* **39** (5), 539–547. 10.1080/00221686.2001.9628278.

Chaudhry, M. H. 2014 *Applied Hydraulic Transients*, 3rd edn. Springer, New York, USA.

Chung, J. Y. & Blaser, D. A. 1980 Transfer function method of measuring in-duct acoustic properties. *I. Theory. J. Acoust. Soc. Am.* **68** (3), 907–913. 10.1121/1.384778.

Covas, D., Ramos, H. & De Almeida, A. B. 2005 Standing wave difference method for leak detection in pipeline systems. *J. Hydraulic Eng.* **131** (12), 1106–1116. 10.1061/(ASCE)0733-9429(2005)131:12(1106).

Duan, H.-F. 2016 Transient frequency response based leak detection in water supply pipeline systems with branched and looped junctions. *J. Hydroinform.* **19** (1), 17–30.

Ghazali, M. F., Beck, S. B. M., Shucksmith, J. D., Boxall, J. B. & Staszewski, W. J. 2012 Comparative study of instantaneous frequency based methods for leak detection in pipeline networks. *Mech. Syst. Signal Pr.* **29**, 187–200. 10.1016/j.ymssp.2011.10.011.

Gong, J., Lambert, M. F., Simpson, A. R. & Zecchin, A. C. 2013a Single-event leak detection in pipeline using first three resonant responses. *J. Hydraulic Eng.* **139** (6), 645–655. 10.1061/(ASCE)HY.1943-7900.0000720.

Gong, J., Simpson, A. R., Lambert, M. F., Zecchin, A. C., Kim, Y.-I. & Tijsseling, A. S. 2013b Detection of distributed deterioration in single pipes using transient reflections. *J. Pipeline Syst. Eng. Prac.* **4** (1), 32–40. 10.1061/(ASCE)PS.1949-1204.0000111.

Gong, J., Stephens, M. L., Arbon, N. S., Zecchin, A. C., Lambert, M. F. & Simpson, A. R. 2015 On-site non-invasive condition assessment for cement mortar-lined metallic pipelines by time-domain fluid transient analysis. *Struct. Health Monit.* **14** (5), 426–438. 10.1177/1475921715591875.

Gong, J., Lambert, M. F., Zecchin, A. C., Simpson, A. R., Arbon, N. S. & Kim, Y.-I. 2016 Field study on non-invasive and non-destructive condition assessment for asbestos cement pipelines by time-domain fluid transient analysis. *Struct. Health Monit.* **15** (1), 113–124. 10.1177/1475921715624505.

Gong, J., Png, G. M., Arkwright, J. W., Papageorgiou, A. W., Cook, P. R., Lambert, M. F., Simpson, A. R. & Zecchin, A. C. 2018 In-pipe fibre optic pressure sensor array for hydraulic transient measurement with application to leak detection. *Measurement* **126**, 309–317. 10.1016/j.measurement.2018.05.072.

Massari, C., Yeh, T. C. J., Ferrante, M., Brunone, B. & Meniconi, S. 2014 Detection and sizing of extended partial blockages in pipelines by means of a stochastic successive linear estimator. *J. Hydroinform.* **16** (2), 248–258. 10.2166/hydro.2013.172.

Meniconi, S., Brunone, B., Ferrante, M. & Massari, C. 2011 Transient tests for locating and sizing illegal branches in pipe systems. *J. Hydroinform.* **13** (3), 334–345. 10.2166/hydro.2011.012.

Meniconi, S., Duan, H. F., Lee, P. J., Brunone, B., Ghidaoui, M. S. & Ferrante, M. 2013 Experimental investigation of coupled frequency and time-domain transient test-based techniques for partial blockage detection in pipelines. *J. Hydraulic Eng.* **139** (10), 1033–1044.

Meniconi, S., Brunone, B., Ferrante, M., Capponi, C., Carrettini, C. A., Chiesa, C., Segalini, D. & Lanfranchi, E. A. 2015 Anomaly pre-localization in distribution–transmission mains by pump trip: preliminary field tests in the Milan pipe system. *J. Hydroinform.* **17** (3), 377–389. 10.2166/hydro.2014.038.

Sattar, A. M., Chaudhry, M. H. & Kassem, A. A. 2008 Partial blockage detection in pipelines by frequency response method. *J. Hydraulic Eng.* **134** (1), 76–89. 10.1061/(ASCE)0733-9429(2008)134:1(76).

Shamloo, H. & Haghighi, A. 2009 Leak detection in pipelines by inverse backward transient analysis. *J. Hydraulic Res.* **47** (3), 311–318.

Sharp, D. B. 1996 *Acoustic Pulse Reflectometry for the Measurement of Musical Wind Instruments.* PhD Dissertation. University of Edinburgh, Edinburgh, UK.

Shi, H., Gong, J., Arkwright, J. W., Papageorgiou, A. W., Lambert, M. F., Simpson, A. R. & Zecchin, A. C. 2015 Transient pressure measurement in pipelines using optical fibre sensor. In: *Proceedings of the 40th Australian Conference on Optical Fibre Technology*. Engineers Australia, Barton, ACT, Australia.

Shi, H., Gong, J., Zecchin, A. C., Lambert, M. F. & Simpson, A. R. 2017 Hydraulic transient wave separation algorithm using a dual-sensor with applications to pipeline condition assessment. *J. Hydroinform.* **19** (5), 752–765. 10.2166/hydro.2017.146.

Soares, A. K., Covas, D. I. C. & Reis, L. F. R. 2011 Leak detection by inverse transient analysis in an experimental PVC pipe system. *J. Hydroinform.* **13** (2), 153–166.

Stephens, M. L., Lambert, M. F. & Simpson, A. R. 2013 Determining the internal wall condition of a water pipeline in the field using an inverse transient model. *J. Hydraulic Eng.* **139** (3), 310–324. 10.1061/(ASCE)HY.1943-7900.0000665.

Wylie, E. B. 1983 The microcomputer and pipeline transients. *J. Hydraulic Eng.* **109** (12), 1723–1739.

Zecchin, A., Lambert, M., Simpson, A. & White, L. 2014 Parameter identification in pipeline networks: transient-based expectation-maximization approach for systems containing unknown boundary conditions. *J. Hydraulic Eng.* **140** (6), 04014020. 10.1061/(ASCE)HY.1943-7900.0000849.

Zeng, W., Gong, J., Zecchin, A. C., Lambert, M. F., Simpson, A. R. & Cazzolato, B. S. 2018 Condition assessment of water pipelines using a modified layer peeling method. *J. Hydraulic Eng.* **144** (12), 04018076. 10.1061/(ASCE)HY.1943-7900.0001547.

Zhang, C., Zecchin, A. C., Lambert, M. F., Gong, J. & Simpson, A. R. 2018 Multi-stage parameter-constraining inverse transient analysis for pipeline condition assessment. *J. Hydroinform.* **20** (2), 281–300. 10.2166/hydro.2018.154.

First received 11 May 2018; accepted in revised form 24 January 2019. Available online 12 February 2019